

# Multi-agent Communication with Graph Information Bottleneck under Limited Bandwidth (a position paper)

Qi Tian

College of Computer Science and Technology, Zhejiang University  
Hangzhou 310058, China

## ABSTRACT

Recent studies have shown that introducing communication between agents can significantly improve overall performance in cooperative Multi-agent reinforcement learning (MARL). In many real-world scenarios, communication can be expensive and the bandwidth of the multi-agent system is subject to certain constraints. Redundant messages who occupy the communication resources can block the transmission of informative messages and thus jeopardize the performance. In this paper, we aim to learn the minimal sufficient communication messages. First, we initiate the communication between agents by a complete graph. Then we introduce the graph information bottleneck (GIB) principle into this complete graph and derive the optimization over graph structures. Based on the optimization, a novel multi-agent communication module, called CommGIB, is proposed, which effectively compresses the structure information and node information in the communication graph to deal with bandwidth-constrained settings. Extensive experiments in Traffic Control and StanCraft II are conducted. The results indicate that the proposed methods can achieve better performance in bandwidth-restricted settings compared with state-of-the-art algorithms, with especially large margins in large-scale multi-agent tasks.

## CCS CONCEPTS

• **Theory of computation** → **Multi-agent reinforcement learning**; • **Mathematics of computing** → **Information theory**.

## KEYWORDS

multi-agent reinforcement learning, bandwidth-constrained communication, information theory

## ACM Reference Format:

Qi Tian. 2018. Multi-agent Communication with Graph Information Bottleneck under Limited Bandwidth (a position paper). In *Woodstock '18: ACM Symposium on Neural Gaze Detection, June 03–05, 2018, Woodstock, NY*. ACM, New York, NY, USA, 10 pages. <https://doi.org/10.1145/1122445.1122456>

## 1 INTRODUCTION

Multi-agent reinforcement learning has shown its powerful ability to cope with many challenging problems, including autonomous

Permission to make digital or hard copies of all or part of this work for personal or classroom use is granted without fee provided that copies are not made or distributed for profit or commercial advantage and that copies bear this notice and the full citation on the first page. Copyrights for components of this work owned by others than ACM must be honored. Abstracting with credit is permitted. To copy otherwise, or republish, to post on servers or to redistribute to lists, requires prior specific permission and/or a fee. Request permissions from [permissions@acm.org](mailto:permissions@acm.org).

Woodstock '18, June 03–05, 2018, Woodstock, NY

© 2018 Association for Computing Machinery.

ACM ISBN 978-1-4503-XXXX-X/18/06...\$15.00

<https://doi.org/10.1145/1122445.1122456>

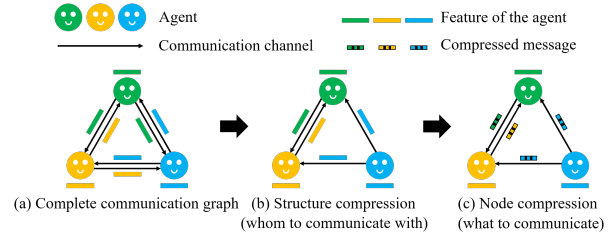


**Figure 1: An illustration of graph structure and node information compression in CGIBNet. (a) A directed complete graph is proposed to model multi-agent communication. (b) Graph structure compression is design for identifying whom to communicate with. (c) Node information compression is used to learn what to communicate.**

driving [24], game playing [25] and swarm robotics [8]. In these scenarios, the communication mechanism is regarded as a promising way to propagate the beliefs of the agents, leading to a better groups' coordination. Thus, a variety of works have been proposed in the field of multi-agent communication to improve the performance of MARL [1, 3, 5, 6, 11, 12, 14, 18, 20, 22, 28].

In real multi-agent systems, however, communication resources are usually limited. Under this setting, the key problem is how to efficiently exploit the available bandwidth and reduce the redundant communication among multi-agents. Hence, we face the following challenges for bandwidth-constrained communication in MARL: (1) **Who to communicate with?** Each agent needs to identify the agents that are necessary to communicate with for a good performance and establish an efficient cooperation protocol among multiple agents. (2) **What to communicate?** Each agent needs to deliver a concise and compact message, otherwise one large message may occupy the whole communication resources.

Recently, many methods [13, 16, 27, 32, 33] have been proposed to address the above challenges, but they have the following shortcomings: 1) Existing methods only focus on one of the challenges, not both. e.g., [13, 16, 27] solve the first challenge, while [32, 33] solve the second. An intuitive idea is to combine these methods to simultaneously overcome the above challenges. However, due to the lack of unified theoretical guidance and some compatibility problems, this combination can only achieve sub-optimal performance. 2) Many previous methods [13, 27, 32] need to learn an extra actor for message aggregation, hence are limited to policy-based MARL frameworks and cannot be applied into value-based MARL frameworks [4]. 3) All methods are designed for single-round communication and cannot compress the communication bandwidth in multiple rounds of communication.

Based on the above discussion, in this paper, we focus on the problem of bandwidth-constrained communication in MARL. To simultaneously address the challenges of whom to communicate with and what to communicate, we propose a novel and universal multi-agent communication model named Communicative Graph Information Bottleneck Network (CGIBNet). Specifically, we first model multi-agent communication with a directed complete graph as is shown in Figure 1(a). Then we derive two optimizable variational upper bounds based on the graph information bottleneck (GIB) principle and instantiate them into two regularizers to compress graph structure and node information. The first regularizer is designed for addressing the challenge of whom to communicate with as is shown in Figure 1(b), by reducing the unnecessary communication channels between agents and maximally preserving information for decision-making. Moreover, in the setting of multi-round communication, this regularizer can also be used in each layer of the graph to reduce communication overhead in each communication round. The second regularizer is designed for solving the problem of what to communicate as is shown in Figure 1(c), by learning compact node representations to reduce bandwidth occupancy. Since the structure learning of CGIBNet is modeled as a link prediction task [35] instead of an actor-based scheduler, our model is learned implicitly with downstream reinforcement learning tasks in an end-to-end manner and can be easily applied to the existing MARL frameworks (*i.e.*, policy-based and value-based MARL). We summarize our contributions as follows:

- We investigate the problem of bandwidth-constrained communication in MARL by simultaneously considering with whom and what to communicate, and give theoretical analysis and optimization surrogate to address this problem through the GIB principle.
- We propose our novel CGIBNet based on the GIB principle, to jointly compress the structure and node information of communication graph for identification of with whom and what to communicate. CGIBNet is a universal module, which can be easily plugged into both policy-based and value-based MARL.
- Experiments on both Traffic Control and StarCraftII show that our proposed method outperforms the state-of-the-art algorithms (including their combination), and the margins are especially large for large-scale multi-agent systems.

## 2 RELATED WORK

**MARL communication.** A variety of works have been proposed to explore communication protocols in MARL, including message aggregation [3, 11, 28], memory-driven communication [20], *etc.* To efficiently utilize finite communication resources, some recent MARL methods introduce various gating mechanisms to reduce communication channels between agents. *e.g.*, IC3Net [27] models the gate by learning an extra actor, while G2A [16] achieves this goal through hard attention and combines with soft attention to improving its performance. However, these methods still need frequent communication. SchedNet [13] leverages a weight generator to explicitly restrict bandwidth occupancy, but this method requires each agent to always communicate with a predefined number of other agents even if the agent can make the optimal decision based

on its own private observation. Also, This method is not suitable for value-based MARL since the generator is modeled as an actor. Another direction is to compress node message representations to save communication resources. *e.g.*, NDQ [33] and IMAC [32] introduce a specific regularizer based on information theory to achieve this goal, but these methods rely on fully connected communication, resulting in sub-optimal message representations and poor performance in some specific scenarios. *e.g.*, target communication is needed [3]. In this paper, we simultaneously schedule communication channels and compress node representations under a unified framework through the graph information bottleneck principle and overcome all their shortcomings.

**Information bottleneck.** Information bottleneck (IB), originally proposed for signal processing, tries to find a short code of the input signal but preserves maximum information of the code [31]. Alemi et al. [2] first introduces the IB into deep neural networks, then the IB is applied to various domains [9, 19, 21]. Recently, Wu et al. [34] extend the IB theory to the graph data to learn compact node representations, which can improve model robustness against adversarial examples. However, they assume that the graph data satisfies the local-dependence assumption and the underlying graph is a static graph, while we deal with a dynamic graph (*i.e.*, communication graph), leading to differences between our method and their method in terms of both theoretical derivation and instantiation.

## 3 PRELIMINARY

In this section, we first introduce the problem setting of MARL communication. Also, we give a brief review of policy-based and value-based MARL with communication since we apply these frameworks for evaluation.

**DEC-POMDP with Communication.** MARL communication is extended from Decentralized Partially Observable Markov Decision Process (Dec-POMDP) and defined as a tuple  $\langle N, \mathcal{S}, \mathcal{A}, \mathcal{T}, \mathcal{R}, \mathbf{O}, \mathbf{M}, \Omega, \gamma \rangle$ , where  $N$  represents the number of agents;  $\mathcal{S}$  represents the state space of the environment;  $\mathcal{A} = \{\mathcal{A}_i\}_{i=1,2,\dots,N}$  represents the set of actions;  $\mathcal{T}(s'|s, \mathbf{a}) : \mathcal{S} \times \mathcal{A} \rightarrow \mathcal{S}$  represents the state transition function and  $\mathbf{a} = [a_1, a_2, \dots, a_N]$  denotes the joint action space;  $\mathcal{R} = \{\mathcal{R}_i\}_{i=1,2,\dots,N} : \mathcal{S} \times \mathcal{A} \rightarrow \mathbb{R}^N$  represents the set of reward functions, and it can be one shared reward in some settings;  $\mathbf{O} = \{\mathcal{O}_i\}_{i=1,2,\dots,N}$  represents the set of local observations for all agents;  $\Omega(s, i) : \mathcal{S} \rightarrow \mathcal{O}_i$  is the observation function that determines the local observation of agent  $i$ ;  $\gamma$  represents the discount factor;  $\mathbf{M} = \{m_i\}_{i=1,2,\dots,N}$  represents the space of messages, where  $m_i$  denotes the message sent by agent  $i$  and it is usually obtained by encoding the local observation  $m_i = \Psi(o_i)$ . Each agent will receive messages  $\mathbf{m}_{-i} = [m_1, \dots, m_{i-1}, m_{i+1}, \dots, m_N]$  sent by its cooperators to make better decisions.

**Policy-based MARL with communication.** Many communication algorithms rely on policy-based MARL. For each agent  $i$ , it aims to directly adjust the parameters  $\theta_i$  of the actor  $\pi_i$  in order to maximize the objective by taking steps in the direction of its gradient. By the policy gradient theorem [29], the gradient of the objective is

$$\nabla_{\theta_i} \mathcal{L}_{MARL,i}^{AC} = \mathbb{E}_{s, a_i \sim \tau} [\nabla_{\theta_i} \log \pi_i(a_i | o_i, \mathbf{m}_{-i}) Q_i(s, \mathbf{a})], \quad (1)$$

where  $\tau$  is the trajectory distribution. We choose one-step TD learning [30] to estimate  $Q_i(s, \mathbf{a})$  in this paper. *i.e.*,  $Q_i(s, \mathbf{a}) = r_i + \gamma V^- (s', \mathbf{a}') - V(s, \mathbf{a})$ , where  $(\cdot)^-$  denotes the target model,  $(\cdot)'$  denotes the corresponding variable at the next timestep. Since  $Q_i$  is used as a critic to criticize the actions made by the actor  $\pi_i$ , the overall algorithm is called Actor-Critic algorithm.

**Value-based MARL with communication.** QMIX [23] is one of the most successful works in value-based MARL, and we choose this method as one of the basic frameworks for multi-agent communication in this paper. QMIX learns a decentralized action-value function  $Q_i$  for each agent and uses a mixing network to combine these local Q values into a global action-value function  $Q_{total}$ . The total loss of QMIX can be denoted as

$$\mathcal{L}_{MARL}^{QMIX} = (r + \gamma \max_{\mathbf{a}'} Q_{total}^-(s', \mathbf{a}') - Q_{total}(s, \mathbf{a}))^2, \quad (2)$$

where  $r$  denotes a cooperative reward. The message  $\mathbf{m}_{-i}$  is used as the input of  $Q_i(o_i, \mathbf{m}_{-i}, a_i)$  in this framework.

## 4 METHODOLOGY

In this section, we first detail the GIB principle in MARL communication to show its mechanism of saving communication resources. Based on the GIB principle, we propose a novel communication model (CGIBNet). Then, we introduce our method to plug CGIBNet into both policy-based and value-based frameworks.

### 4.1 GIB principle in MARL communication

Our work focuses on how to learn a communication model to determine what messages to send and whom to address them in bandwidth-restricted settings. In order to simultaneously solve these two problems under a unified framework, we first model multi-agent communication as a graph, where nodes represent agents and edges represent communication channels between agents. Therefore, the communication process can be regarded as the message passing [7] of each node information under the current graph structure. Without loss of generality, we assume that there are  $L$  rounds of communication between agents [17] so that the communication graph has  $L$  layers. Then the structural representation  $m_S^{(l)}$  and the node representation  $m_X^{(l)}$  at the  $l$ -th layer can be denoted as

$$\begin{aligned} m_S^{(l)} &= \{m_{S,e}^{(l)}, m_{S,e}^{(l)} \in \{0, 1\} \text{ and } e \in \mathcal{E}\} \\ m_X^{(l)} &= \{m_{X,v}^{(l)}, m_{X,v}^{(l)} \in \mathbb{R}^d \text{ and } v \in \mathcal{V}\}, \end{aligned}$$

where  $\mathcal{E}$  and  $\mathcal{V}$  indicate the valid edge set and the node set at the  $l$ -th layer, 0 and 1 indicate the existence of the corresponding edge,  $d$  indicates the dimension of the node representation or the number of bits of each node message [33].

Under the above definition, reducing the bandwidth of multi-agent communication is equivalent to compressing the flow of structural information and node information in the communication graph. The former leads to fewer edge connections and the latter means that fewer bits can be used to express the whole node information.

Inspired by the information bottleneck (IB) principle [2], which is an information-theoretic principle that extracts the minimal sufficient representation for the target task, we extend it to the graph

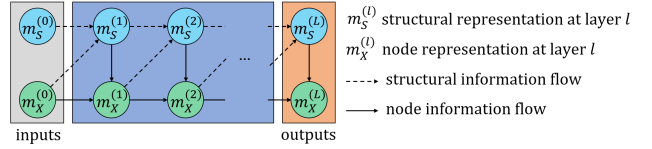


Figure 2: Information flow in the communication graph

information bottleneck (GIB) principle in multi-agent communication. Specifically, we introduce two GIB-based criteria to compress the information flow over graph structures.

The first (minimum) criterion is to respectively constrain the structure-level mutual information  $I(m_S^{(l-1)}; m_S^{(l)})$  and the node-level mutual information  $I(m_X^{(l-1)}; m_X^{(l)})$  between adjacent layers to  $I_S$  and  $I_X$ . This can obtain concise and compact information flow to reduce communication consumption. Considering that we use message passing [7] to propagate the information in the communication graph, the flow of the structural and node information is coupled as is shown in Figure 2. Thus we rewrite the structure-level and node-level mutual information and denote them as structural information bottleneck  $SIB^{(l)}$  and node information bottleneck  $XIB^{(l)}$ , respectively:

$$\begin{aligned} SIB^{(l)} &= I(m_X^{(l-1)}, m_S^{(l-1)}; m_S^{(l)}) < I_S \\ XIB^{(l)} &= I(m_X^{(l-1)}, m_S^{(l)}; m_X^{(l)}) < I_X. \end{aligned}$$

The second (sufficiency) criterion is to maximize the mutual information between all graph representations and the MARL target to preserve task-related information. Since the communication model is jointly trained with other models, it can be achieved by minimizing the MARL task loss.

According to the above analysis, we formulate the GIB principle in bandwidth-limited communication tasks as

$$\begin{aligned} \min \mathcal{L}_{MARL} \\ \text{s.t. } SIB^{(l)} < I_S \text{ and } XIB^{(l)} < I_X, \forall l \in L, \end{aligned} \quad (3)$$

where  $\mathcal{L}_{MARL} \in \{\mathcal{L}_{MARL}^{AC}, \mathcal{L}_{MARL}^{QMIX}\}$  represents the target task loss,  $I_S$  and  $I_X$  limit the amount of information for structural and node representations to decrease bandwidth usage.

In order to facilitate optimization, we use the Lagrangian function to transform Equation (3) into an unconstrained optimization problem

$$\min \mathcal{L}_{MARL} + \beta_S \sum_{l=1}^L SIB^{(l)} + \beta_X \sum_{l=1}^L XIB^{(l)}, \quad (4)$$

where  $\beta_S$  and  $\beta_X$  represent the Lagrangian multipliers that control the compression strength in the optimization. It is notoriously hard to directly optimize  $SIB^{(l)}$  and  $XIB^{(l)}$  due to the intractability of the mutual information terms. Thus we derive their variational upper bounds as is shown in the following theorem.

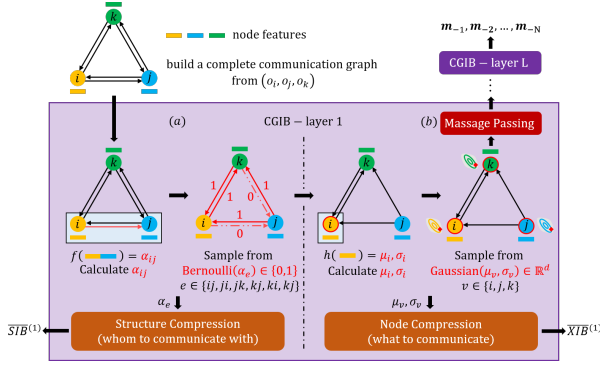


Figure 3: CGIBNet

**THEOREM 1 (UPPER BOUNDS OF  $SIB^{(l)}$  AND  $XIB^{(l)}$ ).** For arbitrary distributions  $r(m_S^{(l)})$  and  $r(m_X^{(l)})$ ,

$$\widehat{SIB}^{(l)} = \mathbb{E}_{m_X^{(l-1)}, m_S^{(l-1)}, m_S^{(l)}} \left[ \log \frac{p(m_S^{(l)} | m_X^{(l-1)}, m_S^{(l-1)})}{r(m_S^{(l)})} \right]$$

$$\widehat{XIB}^{(l)} = \mathbb{E}_{m_X^{(l-1)}, m_S^{(l)}, m_X^{(l)}} \left[ \log \frac{p(m_X^{(l)} | m_X^{(l-1)}, m_S^{(l)})}{r(m_X^{(l)})} \right].$$

The proof of the theorem is deferred to Supplement A. Then substituting Theorem 2 into Equation (4) obtains an optimization surrogate of communication.

## 4.2 Instantiating the GIB principle as CGIBNet

In this section, we propose our novel CGIBNet based on the GIB principle, which leverages two information-theoretic regularizers to solve the problem of with whom and what to communicate in bandwidth-limited communication.

The following corollary illustrates the empirical estimation corresponding to Theorem 2 and the components of CGIBNet are implemented based on it.

**COROLLARY 1 (EMPIRICAL ESTIMATION OF  $\widehat{SIB}^{(l)}$  AND  $\widehat{XIB}^{(l)}$ ).**

$$\widehat{SIB}^{(l)} = \sum_{e \in \mathcal{E}} \text{KL} \left( p_e^{(l)}(m_S^{(l)} | m_X^{(l-1)}, m_S^{(l-1)}) || r(m_S^{(l)}) \right)$$

$$\widehat{XIB}^{(l)} = \sum_{v \in \mathcal{V}} \text{KL} \left( p_v^{(l)}(m_X^{(l)} | m_X^{(l-1)}, m_S^{(l)}) || r(m_X^{(l)}) \right).$$

In the corollary,  $r(m_S^{(l)})$  and  $r(m_X^{(l)})$  are known as the prior structure and the prior node distribution,  $\mathcal{E}$  and  $\mathcal{V}$  represent the valid edge and valid node set at the  $l$ -th layer. The proof of the corollary is deferred to Supplement B.

**Structure compression learning.** In order to calculate  $\widehat{SIB}^{(l)}$  for structural compression, we first focus on the instantiation of  $p_e^{(l)}(\cdot)$ . Specifically, assume that  $m_{X,i}^{(l-1)} \in \mathbb{R}^d$  and  $m_{X,j}^{(l-1)} \in \mathbb{R}^d$  are the node representations of node  $i$  and node  $j$  at the  $(l-1)$ -th layer. Then, we suppose the structural representation  $m_{S,ij}^{(l)} \in \{0, 1\}$  between these two nodes satisfies a Bernoulli distribution, and its

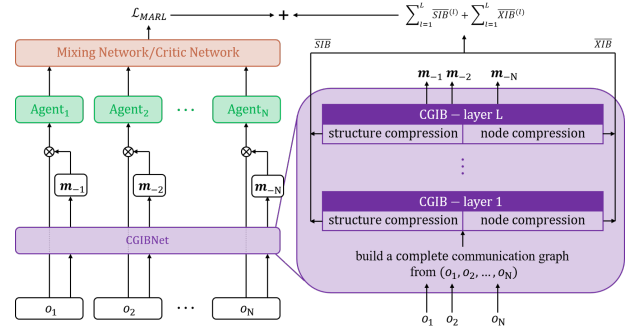


Figure 4: Overall framework of our method

parameter  $\alpha_{ij}^{(l)}$  is calculated as a link prediction task [35]

$$f([m_{X,i}^{(l-1)}; m_{X,j}^{(l-1)}]) \quad (\text{Figure 3(a)})$$

$$= \text{sigmoid}(f_c([m_{X,i}^{(l-1)}; m_{X,j}^{(l-1)}]))$$

$$= \alpha_{ij}^{(l)},$$

where  $[\cdot; \cdot]$  represents vector concatenation and the sigmoid function constrains the output of the link prediction model  $f_c$  to the valid range  $(0, 1)$ . However, it is difficult to back-propagate the gradients if we directly sample  $m_{S,ij}^{(l)}$  from Bernoulli( $\alpha_{ij}^{(l)}$ ). Hence we introduce a relaxed Bernoulli distribution, similar to Jang et al. [10], to solve it, as

$$m_{S,ij}^{(l)} \stackrel{\text{iid}}{\sim} \text{RelaxedBernoulli}(\alpha_{ij}^{(l)}, \tau),$$

where  $\tau \in (0, \infty)$  is the temperature parameter that controls the approximation. When  $\tau$  is close to 0,  $m_{S,ij}^{(l)}$  is approximately sampled from the set  $\{0, 1\}$ .

In the forward stage, the structural representation at the  $l$ -th layer  $m_S^{(l)}$  can be obtained by repeating the process for all valid edges, as is shown in Figure 3(a). In the compression stage, the prior structure distribution  $r(m_S^{(l)})$  in Corollary 1 is set to Bernoulli(0.5) as an uninformative prior. Then incorporating  $\widehat{SIB}^{(l)}$  into Equation (4) indicates that the structure representation can be compressed by minimizing the KL divergence between the posterior distribution  $p_e^{(l)}(\cdot)$  and the prior distribution  $r(m_S^{(l)})$ .

**Node compression learning.** Following previous IB methods [2, 21], we present node embedding as a Gaussian random variable and use the reparameterization trick [15] to tackle the gradient blocking problem. That is, the node message at the  $(l-1)$ -th layer can be obtained as

$$m_{X,v}^{(l-1)} = \mu_v^{(l-1)} \odot \epsilon + \sigma_v^{(l-1)},$$

where  $\odot$  represents the Hadamard product,  $\epsilon$  is sampled from Gaussian(0,  $I$ ). The mean  $\mu_v^{(l-1)} \in \mathbb{R}^d$  and the variance  $\sigma_v^{(l-1)} \in \mathbb{R}^d$  are obtained by the neural network  $h$  (Figure 3(b)), and  $d$  presents the number of bits. Since  $m_S^{(l)}$  has been calculated in the structure learning stage, we can aggregate the information of  $m_X^{(l-1)}$  through message passing. Specifically, assume that node  $i$  at the  $l$ -th layer

needs to receive messages from node  $j$  and node  $k$  according to  $m_S^{(l)}$ . Then we have

$$g([m_{X,i}^{(l-1)}; m_{X,j}^{(l-1)}; m_{X,k}^{(l-1)}]) = m_{X,aggre,i}^{(l)},$$

where  $m_{X,aggre,i}^{(l)}$  will be used as the output of this layer. In the node compression stage, we set the prior node distribution  $r(m_X^{(l)})$  to Gaussian(0,  $I$ ) as is in the previous work [2, 33]. Then it amounts to minimize the current node information bottleneck of each node message to achieve node compression by Corollary 1.

Despite that all bits are maintained during the training process, we desire to discard some of them to satisfy the communication constraints. An important observation is that the current node information bottleneck of each message bit represents the amount of task-related information. An example is that if the current node information bottleneck of all node bits is 0 under the constraint of the node regularizer in Corollary 1, the posterior Gaussian distribution of all bits is equal to the prior Gaussian distribution Gaussian(0,  $I$ ). Since there is no difference between these bits, they do not carry any useful information. On the contrary, if the current node information bottleneck of one bit is large while the other bits are 0, it means that this bit is constrained by  $\mathcal{L}_{MABL}$  and carries most of the task-related information. Therefore, we can rank all bits according to their node information bottleneck, such that bits with smallest amount of information are discarded after the training process.

### 4.3 Apply CGIBNet to MARL framework

Some methods (e.g., IC3Net, SchedNet) schedule the structural representations by learning an additional actor so that these methods are not suitable for value-based MARL frameworks. Instead, we model this task as a link prediction task to perform end-to-end training without other restrictions. Therefore, our CGIBNet model can be plugged into both policy-based and value-based MARL frameworks as is shown in Figure 4. For the value-based method,  $\mathcal{L}_{MABL}$  in Equation (4) represents  $\mathcal{L}_{MABL}^{QMIX}$ , and its calculation follows Equation (2). In this case, Agent $_i$  in Figure 4 represents each individual  $Q_i$  function, and MixingNetwork  $Q_{tot}$  is used to aggregate global information. Similarly, for the policy-based method,  $\mathcal{L}_{MABL}$  in Equation (4) represents  $\mathcal{L}_{MABL}^{AC}$ , and its calculation follows Equation (1). In this case, Agent $_i$  in Figure 4 represents each individual actor  $\pi_i$ , and CriticNetwork  $V$  is used to aggregate global information. See Supplement C for the pseudo-code of CGIBNet.

## REFERENCES

- [1] S Ahilan and P Dayan. 2021. Correcting Experience Replay for Multi-Agent Communication. In *ICLR*.
- [2] Alexander A Alemi, Ian Fischer, Joshua V Dillon, and Kevin Murphy. 2017. Deep variational information bottleneck. In *ICLR*.
- [3] Abhishek Das, Théophile Gervet, Joshua Romoff, Dhruv Batra, Devi Parikh, Mike Rabbat, and Joelle Pineau. 2019. Tarmac: Targeted multi-agent communication. In *ICML*.
- [4] Ali Dorri, Salil S Kanhere, and Raja Jurdak. 2018. Multi-agent systems: A survey. *Ieee Access* 6 (2018), 28573–28593.
- [5] Yali Du, Yifan Zhao, Meng Fang, Jun Wang, Gangyan Xu, and Haifeng Zhang. 2020. Learning Predictive Communication by Imagination in Networked System Control. (2020).
- [6] Jakob N Foerster, Yannis M Assael, Nando de Freitas, and Shimon Whiteson. 2016. Learning to communicate with deep multi-agent reinforcement learning. In *NeurIPS*.
- [7] Justin Gilmer, Samuel S Schoenholz, Patrick F Riley, Oriol Vinyals, and George E Dahl. 2017. Neural message passing for quantum chemistry. In *ICML*.
- [8] Maximilian Hüttenrauch, Sosic Adrian, Gerhard Neumann, et al. 2019. Deep reinforcement learning for swarm systems. *Journal of Machine Learning Research* 20, 54 (2019), 1–31.
- [9] Maximilian Igl, Kamil Ciosek, Yingzhen Li, Sebastian Tschiatschek, Cheng Zhang, Sam Devlin, and Katja Hofmann. 2019. Generalization in Reinforcement Learning with Selective Noise Injection and Information Bottleneck. In *NeurIPS*.
- [10] Eric Jang, Shixiang Gu, and Ben Poole. 2017. Categorical reparameterization with gumbel-softmax. In *ICLR*.
- [11] Jiechuan Jiang, Chen Dun, Tiejun Huang, and Zongqing Lu. 2020. Graph Convolutional Reinforcement Learning. In *ICLR*.
- [12] Jiechuan Jiang and Zongqing Lu. 2018. Learning Attentional Communication for Multi-Agent Cooperation. In *NeurIPS*.
- [13] Daewoo Kim, Sangwoo Moon, David Hostallero, Wan Ju Kang, Taeyoung Lee, Kyunghwan Son, and Yung Yi. 2019. Learning to Schedule Communication in Multi-agent Reinforcement Learning. In *ICLR*.
- [14] Woojun Kim, Jongeui Park, and Youngchul Sung. 2021. Communication in Multi-Agent Reinforcement Learning: Intention Sharing. In *ICLR*.
- [15] Diederik P Kingma and Max Welling. 2014. Auto-encoding variational bayes. In *ICLR*.
- [16] Yong Liu, Weixun Wang, Yujing Hu, Jianye Hao, Xingguo Chen, and Yang Gao. 2020. Multi-agent game abstraction via graph attention neural network. In *AAAI*.
- [17] Georgios Papoudakis, Filippos Christianos, Arrasy Rahman, and Stefano V Albrecht. 2019. Dealing with non-stationarity in multi-agent deep reinforcement learning. *arXiv preprint arXiv:1906.04737* (2019).
- [18] Peng Peng, Ying Wen, Yaodong Yang, Quan Yuan, Zhenkun Tang, Haitao Long, and Jun Wang. 2017. Multiagent bidirectionally-coordinated nets: Emergence of human-level coordination in learning to play starcraft combat games. *arXiv:1703.10069* (2017).
- [19] Xue Bin Peng, Angjoo Kanazawa, Sam Toyer, Pieter Abbeel, and Sergey Levine. 2018. Variational Discriminator Bottleneck: Improving Imitation Learning, Inverse RL, and GANs by Constraining Information Flow. In *ICLR*.
- [20] Emanuele Pesce and Giovanni Montana. 2020. Improving coordination in small-scale multi-agent deep reinforcement learning through memory-driven communication. *Machine Learning* (2020), 1–21.
- [21] Kaizhi Qian, Yang Zhang, Shiyu Chang, Mark Hasegawa-Johnson, and David Cox. 2020. Unsupervised speech decomposition via triple information bottleneck. In *ICML*.
- [22] M Rangwala and R Williams. 2020. Learning Multi-Agent Communication through Structured Attentive Reasoning. In *NeurIPS*.
- [23] Tabish Rashid, Mikayel Samvelyan, Christian Schroeder, Gregory Farquhar, Jakob Foerster, and Shimon Whiteson. 2018. Qmix: Monotonic value function factorization for deep multi-agent reinforcement learning. In *ICML*.
- [24] Ahmad EL Sallab, Mohammed Abdou, Etienne Perot, and Senthil Yogamani. 2017. Deep reinforcement learning framework for autonomous driving. *Electronic Imaging* 2017, 19 (2017), 70–76.
- [25] Mikayel Samvelyan, Tabish Rashid, Christian Schröder de Witt, Gregory Farquhar, Nantas Nardelli, Tim GJ Rudner, Chia-Man Hung, Philip HS Torr, Jakob N Foerster, and Shimon Whiteson. 2019. The StarCraft Multi-Agent Challenge. In *AAMAS*.
- [26] Ohad Shamir, Sivan Sabato, and Naftali Tishby. 2010. Learning and generalization with the information bottleneck. *Theoretical Computer Science* 411, 29-30 (2010), 2696–2711.
- [27] Amanpreet Singh, Tushar Jain, and Sainbayar Sukhbaatar. 2018. Learning when to Communicate at Scale in Multiagent Cooperative and Competitive Tasks. In *ICLR*.
- [28] Sainbayar Sukhbaatar, Arthur Szlam, and Rob Fergus. 2016. Learning multiagent communication with backpropagation. In *NeurIPS*.
- [29] Richard S Sutton, David A McAllester, Satinder P Singh, and Yishay Mansour. 2000. Policy gradient methods for reinforcement learning with function approximation. In *NeurIPS*.
- [30] Gerald Tesauro et al. 1995. Temporal difference learning and TD-Gammon. *Commun. ACM* 38, 3 (1995), 58–68.
- [31] Naftali Tishby, Fernando C Pereira, and William Bialek. 1999. The information bottleneck method. In *Proc. 37th Annual Allerton Conference on Communications, Control and Computing, 1999*.
- [32] Rundong Wang, Xu He, Runsheng Yu, Wei Qiu, Bo An, and Zinovi Rabinovich. 2020. Learning efficient multi-agent communication: An information bottleneck approach. In *ICML*.
- [33] Tonghan Wang, Jianhao Wang, Chongyi Zheng, and Chongjie Zhang. 2020. Learning Nearly Decomposable Value Functions Via Communication Minimization. In *ICLR*.
- [34] Tailin Wu, Hongyu Ren, Pan Li, and Jure Leskovec. 2020. Graph Information Bottleneck. In *NeurIPS*.
- [35] Muhun Zhang and Yixin Chen. 2018. Link prediction based on graph neural networks. In *NeurIPS*.

## 5 SUPPLEMENT

### 5.1 A. Proof for Theorem 1

THEOREM 2 (UPPER BOUNDS OF  $SIB^{(l)}$  AND  $XIB^{(l)}$ ). For arbitrary distributions  $r(m_S^{(l)})$  and  $r(m_X^{(l)})$ ,

$$\begin{aligned}\widehat{SIB}^{(l)} &= \mathbb{E}_{m_X^{(l-1)}, m_S^{(l-1)}, m_S^{(l)}} \left[ \log \frac{p(m_S^{(l)} | m_X^{(l-1)}, m_S^{(l-1)})}{r(m_S^{(l)})} \right] \\ \widehat{XIB}^{(l)} &= \mathbb{E}_{m_X^{(l-1)}, m_S^{(l)}, m_X^{(l)}} \left[ \log \frac{p(m_X^{(l)} | m_X^{(l-1)}, m_S^{(l)})}{r(m_X^{(l)})} \right].\end{aligned}$$

*Proof.* We first derive the structural information bottleneck  $SIB^{(l)}$  as

$$\begin{aligned}SIB^{(l)} &= I(m_X^{(l-1)}, m_S^{(l-1)}; m_S^{(l)}) \\ &= \int_{m_X^{(l-1)}} \int_{m_S^{(l-1)}} \int_{m_S^{(l)}} p(m_X^{(l-1)}, m_S^{(l-1)}, m_S^{(l)}) \log \left( \frac{p(m_X^{(l-1)}, m_S^{(l-1)}, m_S^{(l)})}{p(m_X^{(l-1)}, m_S^{(l-1)}) p(m_S^{(l)})} \right) dm_X^{(l-1)} dm_S^{(l-1)} dm_S^{(l)} \\ &= \int_{m_X^{(l-1)}} \int_{m_S^{(l-1)}} \int_{m_S^{(l)}} p(m_X^{(l-1)}, m_S^{(l-1)}, m_S^{(l)}) \log \left( \frac{p(m_S^{(l)} | m_X^{(l-1)}, m_S^{(l-1)}) p(m_X^{(l-1)}, m_S^{(l-1)})}{p(m_X^{(l-1)}, m_S^{(l-1)}) p(m_S^{(l)})} \right) dm_X^{(l-1)} dm_S^{(l-1)} dm_S^{(l)} \\ &= \int_{m_X^{(l-1)}} \int_{m_S^{(l-1)}} \int_{m_S^{(l)}} p(m_X^{(l-1)}, m_S^{(l-1)}, m_S^{(l)}) \log \left( \frac{p(m_S^{(l)} | m_X^{(l-1)}, m_S^{(l-1)})}{p(m_S^{(l)})} \right) dm_X^{(l-1)} dm_S^{(l-1)} dm_S^{(l)} \quad (5) \\ &= \int_{m_X^{(l-1)}} \int_{m_S^{(l-1)}} \int_{m_S^{(l)}} p(m_X^{(l-1)}, m_S^{(l-1)}, m_S^{(l)}) \log p(m_S^{(l)} | m_X^{(l-1)}, m_S^{(l-1)}) dm_X^{(l-1)} dm_S^{(l-1)} dm_S^{(l)} \\ &\quad - \int_{m_X^{(l-1)}} \int_{m_S^{(l-1)}} \int_{m_S^{(l)}} p(m_X^{(l-1)}, m_S^{(l-1)}, m_S^{(l)}) \log p(m_S^{(l)}) dm_X^{(l-1)} dm_S^{(l-1)} dm_S^{(l)} \\ &= \int_{m_X^{(l-1)}} \int_{m_S^{(l-1)}} \int_{m_S^{(l)}} p(m_X^{(l-1)}, m_S^{(l-1)}, m_S^{(l)}) \log p(m_S^{(l)} | m_X^{(l-1)}, m_S^{(l-1)}) dm_X^{(l-1)} dm_S^{(l-1)} dm_S^{(l)} \\ &\quad - \int_{m_S^{(l)}} p(m_S^{(l)}) \log p(m_S^{(l)}) dm_S^{(l)}.\end{aligned}$$

However, it is difficult to compute the marginal distribution  $p(m_S^{(l)})$ , so let  $r(m_S^{(l)})$  be a variational approximation to this marginal. Then we have

$$\begin{aligned}KL \left[ p(m_S^{(l)}), r(m_S^{(l)}) \right] &\geq 0 \\ - \int_{m_S^{(l)}} p(m_S^{(l)}) \log p(m_S^{(l)}) dm_S^{(l)} &\leq - \int_{m_S^{(l)}} r(m_S^{(l)}) \log r(m_S^{(l)}) dm_S^{(l)}.\end{aligned} \quad (6)$$

Substituting Equation (6) into Equation (5), we have

$$\begin{aligned}SIB^{(l)} &\leq \int_{m_X^{(l-1)}} \int_{m_S^{(l-1)}} \int_{m_S^{(l)}} p(m_X^{(l-1)}, m_S^{(l-1)}, m_S^{(l)}) \log p(m_S^{(l)} | m_X^{(l-1)}, m_S^{(l-1)}) dm_X^{(l-1)} dm_S^{(l-1)} dm_S^{(l)} \\ &\quad - \int_{m_S^{(l)}} r(m_S^{(l)}) \log r(m_S^{(l)}) dm_S^{(l)} \\ &\leq \int_{m_X^{(l-1)}} \int_{m_S^{(l-1)}} \int_{m_S^{(l)}} p(m_X^{(l-1)}, m_S^{(l-1)}, m_S^{(l)}) \log \left( \frac{p(m_S^{(l)} | m_X^{(l-1)}, m_S^{(l-1)})}{r(m_S^{(l)})} \right) dm_X^{(l-1)} dm_S^{(l-1)} dm_S^{(l)} \\ &\leq \mathbb{E}_{m_X^{(l-1)}, m_S^{(l-1)}, m_S^{(l)} \sim p(m_X^{(l-1)}, m_S^{(l-1)}, m_S^{(l)})} \left[ \frac{p(m_S^{(l)} | m_X^{(l-1)}, m_S^{(l-1)})}{r(m_S^{(l)})} \right].\end{aligned}$$

Thus the upper bound of  $SIB^{(l)}$  can be written as

$$\widehat{SIB}^{(l)} = \mathbb{E}_{m_X^{(l-1)}, m_S^{(l-1)}, m_S^{(l)} \sim p(m_X^{(l-1)}, m_S^{(l-1)}, m_S^{(l)})} \left[ \frac{p(m_S^{(l)} | m_X^{(l-1)}, m_S^{(l-1)})}{r(m_S^{(l)})} \right].$$

Similarly, we can get the upper bound of  $XIB^{(l)}$  by replacing the above variables  $m_S^{(l-1)} \rightarrow m_S^{(l)}$  and  $m_S^{(l)} \rightarrow m_X^{(l)}$ , then we have

$$\widehat{XIB}^{(l)} = \mathbb{E}_{m_X^{(l-1)}, m_S^{(l)}, m_X^{(l)} \sim p(m_X^{(l-1)}, m_S^{(l)}, m_X^{(l)})} \left[ \log \frac{p(m_X^{(l)} | m_X^{(l-1)}, m_S^{(l)})}{r(m_X^{(l)})} \right].$$

## 5.2 B. Proof for Corollary 1

COROLLARY 2 (EMPIRICAL ESTIMATION OF  $\widehat{SIB}^{(l)}$  AND  $\widehat{XIB}^{(l)}$ ).

$$\begin{aligned} \overline{SIB}^{(l)} &= \sum_{e \in \mathcal{E}} \text{KL} \left( p_e^{(l)}(m_S^{(l)} | m_X^{(l-1)}, m_S^{(l-1)}) || r(m_S^{(l)}) \right) \\ \overline{XIB}^{(l)} &= \sum_{v \in \mathcal{V}} \text{KL} \left( p_v^{(l)}(m_X^{(l)} | m_X^{(l-1)}, m_S^{(l)}) || r(m_X^{(l)}) \right). \end{aligned}$$

*Proof.* According to Theorem 2, we can obtain the upper bounds  $\widehat{SIB}^{(l)}$  and  $\widehat{XIB}^{(l)}$ . Based on them, we first derive the empirical estimate of  $\overline{SIB}^{(l)}$  as

$$\begin{aligned} \widehat{SIB}^{(l)} &= \mathbb{E}_{m_X^{(l-1)}, m_S^{(l-1)}, m_S^{(l)} \sim p(m_X^{(l-1)}, m_S^{(l-1)}, m_S^{(l)})} \left[ \frac{p(m_S^{(l)} | m_X^{(l-1)}, m_S^{(l-1)})}{r(m_S^{(l)})} \right] \\ &= \int_{m_X^{(l-1)}} \int_{m_S^{(l-1)}} \int_{m_S^{(l)}} p(m_X^{(l-1)}, m_S^{(l-1)}, m_S^{(l)}) \log \left( \frac{p(m_S^{(l)} | m_X^{(l-1)}, m_S^{(l-1)})}{r(m_S^{(l)})} \right) dm_X^{(l-1)} dm_S^{(l-1)} dm_S^{(l)} \\ &= \int_{m_X^{(l-1)}} \int_{m_S^{(l-1)}} \int_{m_S^{(l)}} p(m_X^{(l-1)}, m_S^{(l-1)}) p(m_S^{(l)} | m_X^{(l-1)}, m_S^{(l-1)}) \log \left( \frac{p(m_S^{(l)} | m_X^{(l-1)}, m_S^{(l-1)})}{r(m_S^{(l)})} \right) dm_X^{(l-1)} dm_S^{(l-1)} dm_S^{(l)} \\ &= \int_{m_X^{(l-1)}} \int_{m_S^{(l-1)}} \int_{m_S^{(l)}} p(m_X^{(l-1)}, m_S^{(l-1)}) \text{KL} \left[ p(m_S^{(l)} | m_X^{(l-1)}, m_S^{(l-1)}) || r(m_S^{(l)}) \right] dm_X^{(l-1)} dm_S^{(l-1)} dm_S^{(l)} \\ &= \mathbb{E}_{m_X^{(l-1)}, m_S^{(l-1)} \sim p(m_X^{(l-1)}, m_S^{(l-1)})} \text{KL} \left[ p(m_S^{(l)} | m_X^{(l-1)}, m_S^{(l-1)}) || r(m_S^{(l)}) \right]. \end{aligned} \tag{7}$$

In order to calculate the KL divergence in Equation (7), we need to sample  $m_X^{(l-1)}$  and  $m_S^{(l-1)}$  at the  $(l-1)$ -th layer to calculate the valid structural representation  $m_S^{(l)}$  at the  $l$ -th layer. After  $m_S^{(l)}$  is obtained, the empirical estimation of  $SIB^{(l)}$  can be denoted as

$$\overline{SIB}^{(l)} = \sum_{e \in \mathcal{E}} \text{KL} \left( p_e^{(l)}(m_S^{(l)} | m_X^{(l-1)}, m_S^{(l-1)}) || r(m_S^{(l)}) \right),$$

where  $\mathcal{E}$  represents the valid edge set at the  $l$ -th layer. Similarly, we can get the empirical estimation of  $XIB^{(l)}$  by replacing the above variables  $m_S^{(l-1)} \rightarrow m_S^{(l)}$  and  $m_S^{(l)} \rightarrow m_X^{(l)}$ , then we have

$$\overline{XIB}^{(l)} = \sum_{v \in \mathcal{V}} \text{KL} \left( p_v^{(l)}(m_X^{(l)} | m_X^{(l-1)}, m_S^{(l)}) || r(m_X^{(l)}) \right),$$

where  $\mathcal{V}$  represents the valid node set at the  $l$ -th layer.

### 5.3 C. The pseudo-code of CGIBNet

---

**Algorithm 1** Communicative Graph information Bottleneck Network (CGIBNet)
 

---

**Inputs:** Local observation of each agent ( $o_1, o_2, \dots, o_N$ ), alive mask of each agent ( $al_1, al_2, \dots, al_N$ )

**Neural networks:** Edge network  $f$ , node network  $h$ , aggregation network  $g$

**Hyperparameters:** The number of communication rounds  $L$ , the temperature coefficient in relaxed Bernoulli distribution  $\tau$

**Outputs:** The message received by each agent ( $\mathbf{m}_{-1}, \mathbf{m}_{-2}, \dots, \mathbf{m}_{-N}$ ), structural information bottleneck  $\overline{SIB}$ , node information bottleneck  $\overline{XIB}$

```

1: Let the edge set  $\mathcal{E} = \{m_{S,ij} = 1, 1 \leq i, j \leq N\}$ , the node set  $\mathcal{V} = \{m_{X,i} = o_i, 1 \leq i \leq N\}$ ,  $\overline{SIB} = 0$ ,  $\overline{XIB} = 0$ 
2: # Only alive agents can participate in the communication process
3: for  $n = 1, 2, \dots, N$  do
4:   if  $al_n = 0$  then
5:     Change the valid edge set  $m_{S,nk} = 0$  and  $m_{S,kn} = 0$  ( $1 \leq k \leq N$ )
6:     Change the valid node set  $m_{X,n} = \emptyset$ 
7:   end if
8: end for
9: # Communication process
10: for  $l = 1, 2, \dots, L$  do
11:   # Structure compression learning
12:   for  $m_{S,ij} \in \mathcal{E}$  do
13:     if  $m_{S,ij} = 1$  then
14:       Calculate the parameter of the Bernoulli distribution  $\alpha_{ij} = f(m_{X,i}, m_{X,j})$ 
15:       Use  $\alpha_{ij}$  to calculate  $\overline{SIB}_{ij}$  according to Corollary 1
16:       Add all structural information bottlenecks together for gradient propagation  $\overline{SIB} = \overline{SIB} + \overline{SIB}_{ij}$ 
17:       Sample new  $m_{S,ij} \stackrel{\text{iid}}{\sim} \text{RelaxedBernoulli}(\alpha_{ij}, \tau)$ 
18:     end if
19:   end for
20:   # Node compression learning
21:   for  $m_{X,i} \in \mathcal{V}$  do
22:     if  $m_{X,i} \neq \emptyset$  then
23:       Calculate the parameters of the Gaussian distribution  $\mu_i, \sigma_i = h(m_{X,i})$ 
24:       Use  $\mu_i, \sigma_i$  to calculate  $\overline{XIB}_i$  according to Corollary 1
25:       Add all node information bottlenecks together for gradient propagation  $\overline{XIB} = \overline{XIB} + \overline{XIB}_i$ 
26:       Sample new  $m_{X,i} \stackrel{\text{iid}}{\sim} \text{Gaussian}(\mu_i, \sigma_i)$ 
27:     end if
28:   end for
29:   # Message aggregation
30:   for  $m_{X,i} \in \mathcal{V}$  do
31:     Concatenate all current messages together  $cur\_concat = \text{concat}(m_{X,1}, \dots, m_{X,N})$ 
32:     Mask out the corresponding positions that do not send messages to agent  $i$  ( $m_{S,ki} = 0, (1 \leq k \leq N)$ ) in  $cur\_concat$ 
33:     Aggregate messages sent to agent  $i$ , that is,  $m_{X,i} = g(cur\_concat)$ 
34:   end for
35: end for
36: Assign the aggregated messages to the output  $(\mathbf{m}_{-1}, \mathbf{m}_{-2}, \dots, \mathbf{m}_{-N}) = (m_{X,1}, m_{X,2}, \dots, m_{X,N})$ 
37: return  $(\mathbf{m}_{-1}, \mathbf{m}_{-2}, \dots, \mathbf{m}_{-N}), \overline{SIB}, \overline{XIB}$ 

```

---

### 5.4 D. Calculation details about Structure Compression Ratio (SCR) and Message Compression Ratio (MCR)

**Structure Compression Ratio (SCR).** Recall the definition of SCR mentioned in Section 5.1. Let  $N_{e,complete}$  and  $N_{e,compressed}$  denote the number of edges of the communication graph structure without and with structure compression, respectively. Then, SCR is calculated as  $N_{e,complete} - N_{e,compressed} / N_{e,compressed} \times 100\%$ .

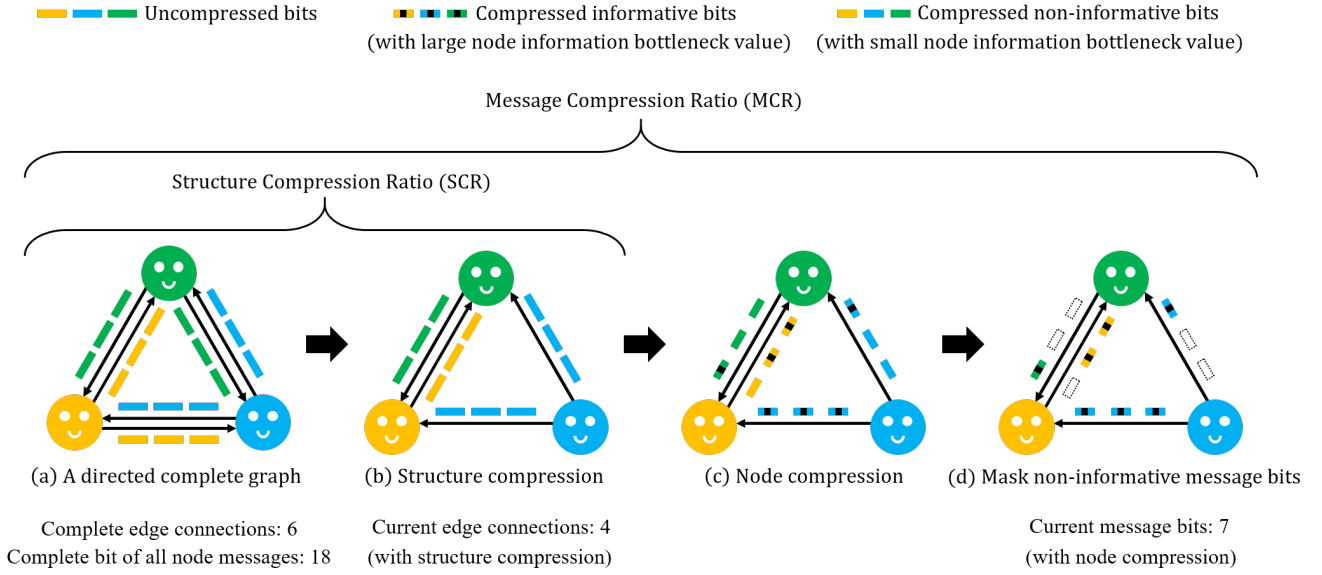


Figure 5: Schematic diagram of calculation of SCR and MCR in CGIBNet

Specifically, as is shown in Figure 8(b), there are 4 edge connections in the communication graph after structure compression, then we have

$$\text{SCR} = \frac{N_{e,complete} - N_{e,compressed}}{N_{e,compressed}} \times 100\% = \frac{6 - 4}{6} = 33.33\%.$$

**Message Compression Ratio (MCR).** Recall the definition of MCR mentioned in Section 5.1. Let  $N_{m,complete}$  denotes the message bits without compression and  $N_{m,compressed}$  denotes the unmasked message bits with compression. Then, MCR is calculated as  $N_{m,complete} - N_{m,compressed} / N_{m,complete} \times 100\%$ .

Specifically, as is shown in Figure 8(c), the information of each bit is compressed after node compression learning and we can judge the importance of these bits based on their node information bottleneck as mentioned in Section 4.2. Figure 8(d) indicates that when the communication bandwidth is constrained, the non-informative bits are masked first. In this case, MCR is calculated as

$$\text{MCR} = \frac{N_{m,complete} - N_{m,compressed}}{N_{m,compressed}} \times 100\% = \frac{18 - 7}{18} = 61.11\%.$$

Since the mask of each bit is implemented as a binary number, it only consumes a negligible log-scale space compared to the length of the message. Also, we adopt diagonal covariance for message embedding in CGIBNet, thus the bits of the node message are uncorrelated and can be masked independently.

## 5.5 E. Environment

### 5.5.1 E.1 Traffic Control.

We take the easy map as an example to detail the implementation of the Traffic Control environment and the mechanism can be extended to medium and hard maps.

**Initialization position.** As is shown in Figure 9(a), each car will be randomly initialized in the colored grid (*i.e.*, straight road), so that they have more opportunities to emerge cooperative behavior in the intersection area.

**Initialization route.** As is shown in Figure 9(b), each car will randomly select one of the two possible routes. one is going straight (*i.e.*, solid line) and is denoted as route 1, the other is turning left (*i.e.*, dotted line) and is denoted as route 2.

**Location coordinates.** As is shown in Figure 9(c), we respectively display the horizontal and vertical coordinates on the map. Therefore, the coordinates of the car can be expressed as  $(4, 5)$ .

**Local observation.** The local observation  $o$  of each car is composed of its location and assigned route id. In order to facilitate network learning, we implement it as a one-hot vector. Specifically, since the location and route id of the car in Figure 9(c) are  $(4, 5)$  and route 2

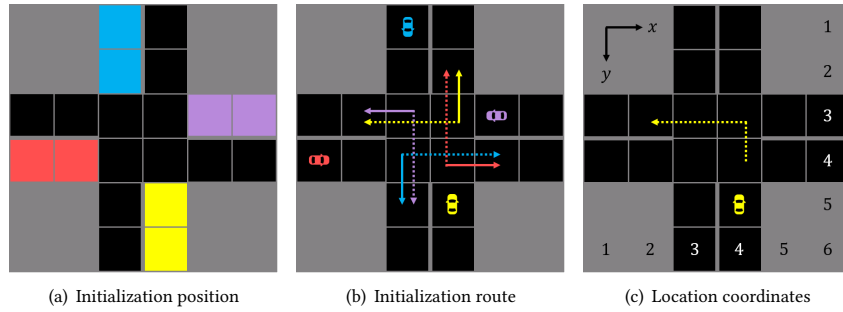


**Figure 6: Experimental details of the easy map in the Traffic Control**

respectively, the local observation  $o$  can be denoted as

$$o = ( \underbrace{0, 0, 0, 1, 0, 0}_{x\text{-axis coordinate}}, \underbrace{0, 0, 0, 0, 1, 0}_{y\text{-axis coordinate}}, \underbrace{0, 1}_{route\ id} ).$$

**Global state.** The global state is a simple concatenation of all local observations.

### 5.5.2 E.2 StarCraftII.



**Figure 7: Snapshots of the StarCraftII scenarios**

StarCraftII micromanagement aims to accurately control the individual units and complete cooperation tasks. In this environment, each enemy unit is controlled by the built-in AI (difficulty level) while each allied unit is controlled by a learned policy. The local observation of each agent contains the following attributes for both allied and enemy units within the sight range: distance, relative\_x, relative\_y, health, shield, and unit\_type. In order to highlight the necessity of communication, we reduce the sight range of each agent from 9 to 2. The action space of each agent includes: noop, move[direction], attack[enemyid], and stop. Under the control of these actions, each agent can move and attack in various maps. The reward setting uses the default reward function, which is based on the hit-point damage dealt on the enemy units, together with special bonuses for killing the enemy units and winning the battle.

**3b\_vs\_1h1m.** As is shown in Figure 10(a), the positions of the 3 Banelings are randomly initialized on the map and they need to kill a Hydralisk that is assisted by a Medivac. 3 Banelings together can just blow up the Hydralisk. Thus they should take action in sync and attack the Hydralisk at the same time, otherwise Medivac will have extra time to heal the Hydralisk, leading to game defeat.

**1o2r\_vs\_4r.** As is shown in Figure 10(b), 1 Overseer has observed 4 enemy Reapers. Allied units of the Observer, 2 Roaches, need to find the Reapers and kill them. Since 1 Overseer and 4 enemy Reapers are initialized at the same location on the map while 2 Roaches are initialized to another location, the Overseer needs to continuously provide the enemy's vision to help 2 allied Roaches find enemy units.

**5z\_vs\_1ul.** As is shown in Figure 10(c), 5 Zealots need to work closely to kill a powerful Ultralisk. Since the sight range of Zealots is severely limited, the communication mechanism can help them to emerge complex cooperation micro-skills.

**1o10b\_vs\_1r.** As is shown in Figure 10(d), this map is full of terrain obstacles, 1 Observer discovers 1 Roach, and its allies, 10 Banelings need to kill this Roach. Similar to the 1o2r\_vs\_4r map, since the initial positions of Overseer and Roach are inconsistent with that of Banelings, the Overseer needs to encode the Roach's location information and send it to the allied Banelings to win the game.